Integrating Saharan dust forecasts into a regional chemical transport model: a case study over Northern Italy

C. Carnevale[1*], G. Finzi[1], E. Pisoni[1], M. Volta[1], P. Kishcha[2], P.Alpert[2]

[1]*Dept. of Information Engineering, Faculty of Engineering, University of Brescia, Italy.*

**Corresponding author: carneval@ing.unibs.it*

[2]*Department of Geophysics and Planetary Sciences, Tel-Aviv University,*

69978 Tel-Aviv, Israel

Abstract

The Po Valley in Northern Italy is frequently affected by high PM10 concentrations, where both natural and anthropogenic sources play a significant role. To improve air pollution modeling, 3D dust fields, produced by means of the DREAM dust forecasts, were integrated as boundary conditions into the mesoscale 3D deterministic Transport Chemical Aerosol Model (TCAM). A case study of the TCAM and DREAM integration was implemented over Northern Italy for the period May 15 – June 30, 2007. First, the Saharan dust impact on PM10 concentration was analyzed for eleven remote PM10 sites with the lowest level of air pollution. These remote sites are the most sensitive to Saharan dust intrusions into Northern Italy, because of the absence of intensive industrial pollution. At these remote sites, the observed maxima in PM10 concentration during dust events is evidence of dust aerosol near the surface in Northern Italy. Comparisons between modeled PM10 concentrations and measurements at 230 PM10 sites in Northern Italy, showed that the integrated TCAM-DREAM model more accurately reproduced PM10 concentration than the base TCAM model, both in terms of correlation and mean error. Specifically, the correlation median increased from 0.40 to 0.65, while the normalized mean absolute error median dropped from 0.5 to 0.4.

Keywords: Aerosol, Saharan dust, Dust forecast, Multiphase chemical transport model.

1. Introduction

According to the EU Directive 2008/50, where exceedance of the pollution limit can be attributed to natural sources rather than to anthropogenic sources, the exceedance can be discounted after scientific validation, by European Union State Members,. In connection with this, in recent years, a number of experimental studies have been performed to investigate the contribution of Saharan dust to PM10 concentrations in the Euro-Mediterranean basin (Gobbi et al., 2007, Escudero et al., 2007, Masson et al., 2010, Perrino et al., 2008, Pederzoli et al., 2010, Rodriguez et al., 2001).

Saharan dust is frequently transported over the Italian Peninsula, especially during the summer season (Pederzoli et al., 2010). Previous studies, based on lidar measurements of dust vertical distribution over Rome, showed that, on average, the dust layer is far from the surface and is located within a wide range of altitude from 0.5 km to 8 km (Kishcha et al., 2005). However, in accordance with recent experimental studies, carried out independently by Gobbi et al. (2007), Perrino et al. (2008), and Pederzoli et al. (2010), some mixing of dust with local aerosols below the dust layer bottom boundary is often highly probable. In particular, on approximately 30% of days in 2001, dust contribution to daily PM10 levels in Rome was estimated at about 20 μg m^{-3} (Gobbi et al., 2007). In accordance with chemical analysis of PM10 measurements in Central Italy, Saharan dust contributes as much as 32 % to the total PM10 mass during dust transport events (Perrino et al., 2008). The contribution of Saharan dust to PM10 monthly concentrations, as much as 8 - 10 μg m^{-3}, was estimated at seven Italian locations, from the Ispra site in North Italy to the Lampedusa site in South Italy (Pederzoli et al., 2010). Therefore, it is essential to give correct model estimates of the contribution of Saharan dust to air quality in Italy.

Regional dust models are considered to be a useful tool for simulating dust contribution to surface aerosol concentration, where dust transport is significant (Kishcha et al., 2008, Papanastasiou et al., 2010, Pederzoli et al., 2010). However, despite the large number of available chemical weather forecasting systems for simulating aerosol contribution to air quality in Europe (http://chemicalweather.eu/Links), few of these models include Saharan dust. On the other hand, multiphase models, simulating the physical-chemical processes involving secondary pollutants in the troposphere, are key tools for evaluating the effectiveness of emission control strategies and thereby for the improvement in air quality. Due to the complexity of phenomena involved in the formation and accumulation of aerosols, these models require detailed input in terms of meteorological fields, emission sources and boundary conditions. If we improve boundary condition fields on Saharan dust transport, we could give information to our mesoscale model about external pollutant fluxes entering the model domain.

This study was aimed at giving better model estimates of air pollution in Northern Italy. Saharan dust forecasts over the Mediterranean region, daily computed at Tel-Aviv University (Kishcha et al., 2008) were used to improve boundary conditions of the mesoscale multiphase Transport Chemical Aerosol Model (TCAM) model, developed at the University of Brescia (Carnevale et al., 2008). Integrating Saharan dust forecasts into TCAM allowed us to obtain better model estimates of PM10 concentration.

2. Modelling System Configuration

Two different configurations of the Gas Aerosol Modeling Evaluation System (GAMES) (Volta and Finzi, 2006) are considered in this study. In the base configuration (Fig. 1), the modeling system includes: the TCAM chemical transport model (Carnevale et al., 2008); the meteorological pre-processor PROMETEO; the emission processor POEM-PM (Carnevale et al., 2006); and a pre-processor computing the boundary conditions on the basis of CHIMERE continental scale simulations (Schmidt et al. 2001). In the second model configuration, Saharan dust forecasts were integrated into the base model system, in order to improve boundary conditions on large-scale transport of dust over the model domain (Fig. 2). In this second model configuration, dust was a passive component: no interaction between dust and other aerosol species was included.

2.1 TCAM model

TCAM is a 3-D multiphase Eulerian model which solves a system of partial differential equations for each time step. TCAM describes horizontal/vertical transport; multiphase chemical reactions; and gas-to-particle conversion phenomena using a splitting operator technique (Marchuk, 1975). Horizontal transport is solved using a chapeau function approximation (Pepper et al., 1979) and a nonlinear Forester filter (Forester, 1977), while the vertical transport PDE system is solved using a hybrid implicit/explicit scheme. Gas chemistry is simulated using a modified version of the SAPRC97 scheme (Carnevale et al., 2010). The ODE chemical kinetic system is solved by means of the Implicit-Explicit Hybrid (IEH) solver (Chock et al., 1994), which splits the species into fast and slow ones, according to their reaction rates. The system of fast species is solved by means of the implicit Livermore Solver for Ordinary Differential Equations (LSODE) (Hindmarsh, 1975) implementing the Adams predictor/corrector method in a non-stiff case and the Backward Differentiation Formula method in a stiff case (Carnevale et al., 2008). The slow species system is solved using the Adams-Bashfort method (Carnevale et al., 2008). The aerosol module simulates the particles by means of a fixed-moving approach. A generic particle is represented by an internal core containing non-volatile material, such as elemental carbon and crustal aerosol. The core dimension of each size class is established at the beginning of the simulation and is held constant during all the computations. The volatile material is assumed to reside in the outer shell of the particle whose dimension is evaluated by the module at each time step, on the basis of the total mass and of the total number of suspended particles. The aerosol module describes the dynamics of 21 chemical compounds: twelve inorganic species (H2O, SO4=, NH4+, Cl−, NO3−, Na+, H+, SO2 (aq), H2O2 (aq), O3 (aq), elemental carbon and others), and 9 organic species consisting of one generic primary organic species and 8 classes of secondary organic species. Each chemical species is split into n (namely n=10) size bins. The inorganic species thermodynamic equilibrium is solved using ISORROPIA-II (Nenes et al., 1998), (Fountoukis and Nenes, 2007), (http://nenes.eas.gatech.edu/ISORROPIA).

The TCAM model has been widely used and validated in the frame of a number of national and international projects (Cuvelier et al., 2007) (Carnevale et al., 2008) (Di Nicolantonio et al. 2009).

2.2 DREAM desert dust forecasts

DREAM is a model designed to predict the atmospheric cycle of mineral dust aerosol (Nickovic et al., 2001). It solves the Euler-type partial differential nonlinear equation for dust mass continuity. The NCEP/Eta regional atmospheric model drives the aerosol. During the model integration, calculations of the surface dust injection fluxes are made over the model cells declared as deserts. DREAM includes dust sources located in the Western, Central, and Eastern Sahara, as well as in the Arabian Peninsula. Wind erosion of the soil in the DREAM parameterization scheme is controlled by several factors, such as the type of soil (soil texture), type of vegetation cover, soil moisture content, and surface atmospheric turbulence. Once injected into the air, dust aerosol is driven by turbulence in the early stage of the process, when dust is lifted from the ground to the upper levels, and subsequently by winds in the later phases of the process, when dust travels away from the sources. DREAM includes processes of wet (Giorgi, 1986) and dry deposition. Eight size bins covering the particle effective sizes from 0.1 μm to 8.0 μm are used in the model.

DREAM has been used for several years for producing operational dust forecasts at Tel-Aviv University, Israel. Several publications on the DREAM model validation against lidar measurements, AERONET data, and PM10 measurements are available (Amiridis et al., 2009, Kishcha et al., 2007, Papanastasiou et al., 2010, Papayannis et al., 2007, Perez et al., 2006). At Tel-Aviv University, since the year 2006, DREAM has been producing daily forecasts of 3-D distribution of dust concentrations over the Mediterranean region, the Middle East, Europe, and the Atlantic Ocean (http://wind.tau.ac.il/dust8/dust.html). In the current study, dust forecasts over the Mediterranean domain (20°W – 45°E, 15°N – 50°N) were used, with horizontal resolution of 0.3° and 24 vertical levels between 86 m and approximately 15 km above the sea level. DREAM is initialized with the NCEP analysis and the lateral boundary data are updated every six hours by the NCEP GFS model. The runs start at 1200 UTC and forecasts are performed for 3-hour periods up to 72 hours ahead. With respect to dust, DREAM is initialized with 3-D dust distributions from previous days.

3. The case study

3.1 Dust event characterization

During the period under consideration in the current study from May 15 to June 30, 2007, four dust events were observed over Northern Italy: May 20 – 29, June 3 – 15, June 18 – 22, June 24 – 26. Figs. 3 and 4 illustrate Saharan dust transport by showing modeled dust distribution; wind vectors, and satellite images with dust. The 3000 m altitude (~ 700 hPa) was chosen for displaying wind vectors because the average transportation of the dust takes place above the humid air of the PBL, between 600–800 hPa (Carlson and Prospero, 1972, Hamonou et al., 1999, Barkan et al., 2005, Alpert et al., 2004). Three of the dust events showed a similar situation with dust close to the surface. However, it should be noted that the dust event on June 3 – 15, 2007, was mainly characterized by dust distant from the surface, which made an insignificant contribution to PM10 concentration (Fig. 3).

The synoptic situation during the aforementioned dust events was characterized as follows:

May 20 – 29, 2007 - in this phenomenon, Saharan dust was transported to Italy simultaneously along two different routes: (a) from the Eastern Sahara (Fig. 3a), and (b) from the Western Sahara (Fig. 3 b). The synoptic situation was characterized by a specific structure consisting of two intensive low-pressure systems, one over the Eastern Mediterranean and the other over the Eastern Atlantic. A strong anticlockwise airflow, associated with the low over the Eastern Mediterranean, transported dust in an anticlockwise movement from the Eastern Sahara, around the Eastern Mediterranean, to Northern Italy (Fig. 3b). Simultaneously, the other low over the Eastern Atlantic produced favorable conditions for the development of a heavy dust storm over the Western Mediterranean, accompanied by dust intrusions into Northern Italy (Fig. 3b). Satellite images with dust over sea areas adjacent to Northern Italy supported model simulations (Fig. 3c).

June 3 – 15, 2007 – the long dust presence over Northern Italy was due to a sequence of dust events. From June 3 – 4, 2007, an intensive low-pressure system over the Central Mediterranean created favorable conditions for dust transport from dust sources in the

Libyan Desert to Italy (Fig. 3d). As this low-pressure system shifted eastward during June 5 – 9, 2007, dust from the eastern part of the Sahara was transported to Northern Italy. A low-pressure system over the tropical east Atlantic, generating south-west winds in its eastern flank, could cause dust transport to Northern Italy from June 10 – 15, 2007. As mentioned above, in accordance with DREAM 3-D dust distributions over Northern Italy, this dust event was mainly characterized by dust distant from the surface, which made an insignificant contribution to PM10 concentration. This is illustrated in Fig. 3e presenting dust distribution within the vertical cross-section along 10.2^{o} longitude. In the second dust event, dust was not seen from space because of cloud cover over Northern Italy and adjacent sea areas (Fig. 3f). Nevertheless, for the sake of consistency, we presented the satellite image for the second dust event, as we did for all other events.

June 18 – 22, 2007 - an intensive Atlantic cyclone was the main causal factor for a severe dust storm over the Western Mediterranean, accompanied by a direct dust transport along the route from North Africa, through Italy, into the Po Valley (Fig. 4a). The modeled dust transport was supported by satellite images with dust (Fig. 4b).

June 24 – 25, 2007 - as a consequence of the aforementioned Atlantic low, an extensive high-pressure system arose over the whole Mediterranean Sea. As a result, a dust storm took place over the Mediterranean, accompanied by dust intrusion into Northern Italy (Fig. 4 c and d).

3.2 Impact on TCAM performances

As mentioned, the impact of DREAM dust boundary conditions on TCAM performance over Northern Italy was assessed by comparing two model configurations, one with and one without DREAM boundary conditions. The TCAM configuration without DREAM boundary conditions is called hereafter the base TCAM model. Both TCAM model configurations were run over the model domain (Fig. 2) with 10 km × 10 km horizontal resolution and 11 vertical levels, from 10m to 4000 m above ground level. Following that, the DREAM dust boundary condition impact on TCAM performance was assessed in terms of correlation and mean normalized model absolute error, by comparing modeled PM10 concentrations with PM10 measurements for the period under investigation.

230 PM10 monitoring sites, scattered all around the model domain (Fig. 2, crosses), were used in order to comprehensively capture the distribution of particulate emissions affecting the domain. At different PM10 sites, PM10 concentrations, averaged over the period under consideration, varied between 10 and 50 $\mu g/m^3$. The sites with the lowest average PM10 concentration are remote from both industrial centers and highly-populated areas. These remote PM10 sites show the minimal level of air pollution in Northern Italy.

3.2.1. TCAM-DREAM performance over remote PM10 sites

It is reasonable to suggest that these remote PM10 sites are most sensitive to Saharan dust intrusions into Northern Italy, because of the absence of intensive industrial pollution.

The dust impact on PM10 concentration at these sites should be noticeable on the background of low PM10 concentrations. Consequently, first we analyzed the Saharan dust impact on TCAM performance for the eleven PM10 sites, whish were characterized by the lowest average PM10 concentrations (PM10 $\leq$ 14 $\mu g/m^3$) over the period under consideration

Fig. 5 represents time series of measured and modeled PM10 concentration averaged over the aforementioned remote sites. It is seen that the observed PM10 concentrations (stars) show two pronounced maxima during the two dust events May 20 – 29 and June 18 – 22, 2007. The PM10 concentrations in these maxima are approximately two times higher than the background PM10 level. At these remote sites, such a strong deviation from the background level can not be attributed to anthropogenic aerosol emissions, because of their distance from anthropogenic sources. Moreover, the base TCAM model was not capable of reproducing the two observed PM10 maxima (Fig. 5), because the dust effect was not included. The two aforementioned facts provided us with evidence of dust aerosol near the surface in Northern Italy. Due to the use of improved boundary conditions, the integrated TCAM-DREAM model more accurately reproduced PM10 measurements than the base TCAM model. For the two other dust events on June 3 – 15 and June 24 – 26, 2007, modeled PM10 concentrations were close to the background PM10 concentrations, in accordance with PM10 measurements.

3.2.2. TCAM-DREAM performance over 230 PM10 sites in Northern Italy

The time series of measured PM10 concentration, averaged over all available 230 PM10 monitoring sites, were obtained for each day from May 15 to June 30, 2007. For the 230 PM10 sites distributed over the model domain, model-vs.-measurement comparisons for both model configurations showed that the use of DREAM boundary conditions led TCAM to better performance (Fig. 6). In particular, the integrated TCAM-DREAM model was able to capture high peaks in measured PM10 concentration during the two dust events, May 20 – 29, and June 18 – 22, 2007. Note that, although the integrated TCAM-DREAM model more accurately reproduced PM10 measurements than the base TCAM model, sometimes there was some discrepancy between modeled concentrations and measurements. Specifically, during the period under consideration, TCAM-DREAM modeled concentrations were somewhat lower than PM10 measurements. In addition, there was a three-day delay between the measured and modeled PM10 maxima during the first dust event on May 21 – 29, 2007 (Fig. 6). A possible reason for the delay could be errors in the meteorological parameters.

The better capability of the integrated TCAM-DREAM model over the base TCAM model is illustrated by the better correspondence of 95th percentiles between observed and modeled PM10 concentration (Fig. 7). To further support this point, the DREAM dust boundary condition impact on TCAM performance was assessed in terms of correlation (r) and normalized mean absolute error (nmae). Fig. 8 represents box-plots of the correlation coefficient (Fig. 8a) and the normalized mean absolute error (Fig. 8b), computed on the basis of model-vs.-measurement comparisons at 230 PM10 monitoring sites. The boxes show a significant increase in the r median from 0.40 to 0.65 achieved by using DREAM dust boundary conditions (Fig. 8a). The nmae median dropped from 0.5 for the base simulation to 0.4 for the simulation with DREAM boundary conditions (Fig. 8b). This result indicates the improvement in model performance due to the use of DREAM boundary conditions.

In order to demonstrate how the improvement in model performance covers the model domain, the difference in correlation between measured and modeled PM10 concentrations, based on the two model configurations, was analyzed (Fig. 9a). The improvement was characterized by a positive correlation difference higher than 0.1. The map of the correlation differences highlights the fact that the noticeable improvement in TCAM model performance was observed almost over the entire model domain. We used a map of name differences in order to demonstrate how the decrease in normalized mean absolute error covers the model domain. The improvement was characterized by a negative nmae difference less than -0.1. Shown in Fig. 9b, the map of nmae differences demonstrates a noticeable improvement in the integrated TCAM-DREAM model performance almost over the entire model domain, achieved by the use of DREAM boundary conditions.

Conclusions

To improve air pollution modeling, 3D dust fields, produced by means of the DREAM dust forecasts, were integrated as boundary conditions into the TCAM chemical transport model. This allowed us to reproduce Saharan dust contribution to PM10 concentration over Northern Italy for the period May 15 – June 30, 2007, when four significant dust events were observed.

First, Saharan dust impact on TCAM performance was analyzed at eleven remote PM10 sites which had the lowest level of air pollution (PM10 $\leq$ 14 $\mu g/m^3$) over the period under consideration. For those remote sites, the observed high PM10 concentrations during dust events stood prominently on the background of low PM10 concentrations. At the remote sites, such a strong deviation from the background level can not be attributed to anthropogenic aerosol emissions because of their distance from anthropogenic sources. The observed maxima in PM10 concentration during dust events is evidence of dust aerosol near the surface in Northern Italy. During all dust events under consideration, the integrated TCAM-DREAM model produced more accurate PM10 concentrations than the base TCAM model.

A comparison between modeled PM10 concentrations and PM10 measurements during the period under study May 15 – June 30, 2007, was carried out at 230 PM10 monitoring sites, distributed within the model domain. This model-vs.-measurement comparison showed that the integrated TCAM –DREAM model more accurately reproduced PM10 concentrations than the base TCAM model, both in term of correlation and mean error. Specifically, as estimated for 230 PM10 monitoring sites, the correlation median increased from 0.40 to 0.65, while the normalized mean absolute error median dropped from 0.5 to 0.4. Noticeable improvement in TCAM model performance was obtained almost over the entire model domain.

The obtained results indicate that dust can contribute significantly to PM10 concentrations in Northern Italy. This dust contribution should be taken into account when estimating the exceedance of pollution limits. Our results are of importance to countries which have to pay a penalty for exceeding the pollution limit. By subtracting dust contribution from PM10 measurements, these countries could show lower rates of man-made pollution.

Acknowledgments

The work has been partially supported by COST ES0602 action and MIUR (Ministero Italiano Università e Ricerca). The authors acknowledge Dr. G. Curci (CETEMPS, Italy) for the Chimere boundary conditions.

References

Alpert P., Kishcha P, Shtivelman A, Krichak S, Joseph J. Vertical distribution of Saharan dust based on 2.5-year model predictions. Atmospheric Research 2004;70: 109–130.

Amiridis V, Kafatos M, Perez C, Kazadzis S, Gerasopoulos E, Mamouri RE, et al. The potential of the synergistic use of passive and active remote sensing measurements for the validation of a regional dust model. Annales Geophysicae 2009;27:3155-3164.

Barkan J, Alpert P, Kutiel H, Kishcha P. Synoptics of dust transportation days from Africa toward Italy and central Europe, J. Geophys. Res. 2005;110, D07208, doi:10.1029/2004JD005222.

Carlson TN, Prospero JM. The large-scale movement of Saharan air outbreaks over the northern equatorial Atlantic, Journal of Applied Meteorology 1972;11: 283–297.

Carnevale C, Gabusi V, Volta M. POEM-PM: an emission model for secondary pollution control scenarios, Environmental Modelling and Software, 2006;21:320-329.

Carnevale C, Decanini E, Volta M. Design and validation of a multiphase 3D model to simulate tropospheric pollution, Science of the Total Environment, 2008;390:166-176.

C. Carnevale, E. Pisoni and M. Volta. A non-linear analysis to detect the origin of PM10 concentrations in Northern Italy, Science of the Total Environment, 2010;409:182-191.

Chock DP, Winkler SL, Sun P. Comparison of Stiff Chemistry Solvers for Air Quality Modeling. Environ. Sci. Technol., 1994;28:1882–1892.

Cuvelier C, Thunis P, Vautard R, Amann M, Bessagnet B, Bedogni M, et al. CityDelta: A model intercomparison study to explore the impact of emission reductions in European cities in 2010. Atmospheric Environment, 2007;41:189-207.

Di Nicolantonio W, Cacciari A, Petritoli A, Carnevale C, Pisoni E, Volta M et al. MODIS and OMI satellite observations supporting air quality monitoring. Radiation Protection Dosimetry, 2009;137:280-287.

Ecudero M, Querol X, Avila A, Cuevas E. Origin of the exceedances of the European daily PM limit value in regional background areas of Spain. Atmospheric Environment, 2007;41:730-744.

Forester C. Higher order monotonic convection difference schemes. Journal of Computational Physics, 1977;23:1–22.

Fountoukis C, Nenes A. ISORROPIA II: A Computationally Efficient Aerosol Thermodynamic Equilibrium Model for K+, Ca2+, Mg2+, NH4+, Na+, SO4=, NO3-, Cl-, H2O Aerosols, Atmospheric Chemistry and Physic, 2007;7:4639–4659.

Giorgi, F. A particle dry-deposition parameterization scheme for use in tracer transport models. J. Geophys. Res., 1986;91:9794–9806.

Gobbi GP, Barnaba F, Ammannato L. Estimating the impact of Saharan dust on the year 2001 PM10 record of Rome, Italy. Atmospheric Environment, 2007;41:261-275.

Hamonou E, Chazette P, Bali D, Dulac F, Schneider X, Galani F, Ancellet G, Papayanis A. Characterization of the vertical structure of the Saharan dust transport to the Mediterranean basin. J. Geophys. Res. 1999;104:256– 270.

Hindmarsh A. LSODE and LSODEI, two new initial value ordinary differential equation solvers, ACM-SIGNUM Newsletter, 1980;15:10–11.

Kishcha P, Barnaba F, Gobbi GP, Alpert P, Shtivelman A, Krichak S et al. Vertical distribution of Saharan dust over Rome (Italy): comparison between 3-year model predictions and lidar soundings. J. Geophys. Res., 2005;110.

Kishcha P, Alpert P, Shtivelman A, Krichak S, Joseph J, Kallos G et al. Forecast errors in dust vertical distributions over Rome (Italy): Multiple particle size representation and cloud contributions. J. Geophys. Res., 2007;112.

Kishcha P, Nickovic S, Ganor E, Kordova L, Alpert P. Saharan dust over the Eastern Mediterranean: Model sensitivity. Air pollution modelling and its applications XIX. 2008;4:358-366.

Marchuk G. Methods of Numerical Mathematics, Springer-Verlag, New York; 1975.

Masson O, Piga D, Guarriaran R, D'Amico D. Impact of exceptional Saharan dust outbreak in France: PM10 and artificial radionuclides concentrations in air in dust deposit. Atmospheric Environmnet, 2010;44: 2478-2486.

Nenes A, Pandis S, Pilinis C. ISORROPIA: A new thermodynamic equilibrium model for multiphase multicomponent inorganic aerosols. Aquatic Geochemistry, 1998;4:123-152.

Nickovic S, Kallos G, Papadopoulos A, Kakaliagou O. A model for prediction of desert dust cycle in the atmosphere. J. Geophys. Res., 2001;106:18113-18129.

Papanastasiou DK, Poupkou A, Katragkou E, Amiridis V, Melas D, Mihalopoulos N et al. An assessment of the efficiency of dust regional modelling to predict Saharan dust transport episodes. Advances in Meteorology, 2010;doi:10.1155/2010/154368.

Papayannis A, Zhang H, Amiridis V, Ju H, Chourdakis G, Georgoussis G et al. Extraordinary dust event over Beijing, China, during April 2006: Lidar, Sun photometric, satellite observations and model validation. Geophys. Res. Let., 2007;34:doi:10.1029/2006GL029125.

Pederzoli A, Mircea M, Finardi S, Di Sarra A, Zanini G. Quantification of Saharan dust contribution to PM10 concentrations over Italy during 2003 – 2005. Atmospheric Environment, 2010;44:4181-4190.

Pepper D, Kern C, Long P. Modelling the dispersion of atmospheric pollution using cubic splines and chapeau functions, Atmospheric Environment, 1979;13:223–237.

Pérez C, Nickovic S, Pejanovic G, Baldasano JM, Özsoy E. A long Saharan dust event over the western Mediterranean: Lidar, sun photometer observations and regional dust modeling. J. Geophys. Res., 2006;111: D15214, doi:10.1029/2005JD006579.

Perrino C, Canepari S, Cardarelli E, Catrambone M, Sagolini T. Inorganic constituents of urban air pollution in the Lazio region (Central Italy). Environmental Monitoring and Assessment, 2008;136:69-86.

Rodriguez S, Querol X, Alastuey A, Kallos, G, Kakaliagou O. Saharan dust contributions to PM10 and TSP levels in Southern and Eastern Spain, Atmospheric Environment, 2001;35:2433-2447.

Schmidt H, Derognat C, Vautard R, Beekman M. A comparison of simulated and observed ozone mixing ratios for the summer of 1998 in Western Europe. Atmospheric Environment, 2001;35:6277–6297.

Volta M, Finzi G. GAMES, a comprehensive gas aerosol modelling evaluation system, Environmental Modelling and Software, 2006;21;587-594.

Figure captions

Fig. 1. The TCAM model configuration with embedded DREAM dust forecasts.

Fig. 2. The Northern Italy model domain with PM10 monitoring sites (crosses). The red rings designate the remote PM10 sites with the lowest average PM10 concentration.

Fig. 3. DREAM dust forecasts and SeaWIFS satellite images of Saharan dust transport to Northern Italy in the first (top) and second (bottom) dust events. In Fig. 3 a, b, and d the colors designate dust loading in g/m2, while in Fig. 3e the colors designate dust concentration in μg/m3 within the vertical cross-section along the 10.2o longitude. Wind vectors designate wind at 3000 m altitude.

Fig. 4. DREAM dust forecasts (left panel) and SeaWIFS satellite images (right panel) of Saharan dust transport to Northern Italy: (a and b) June 19, 2007, and (c and d) June 24, 2007. In the left panel, the colors designate dust loading in g/m^2, while wind vectors designate wind at 3000 m altitude.

Fig. 5. Time series of measured and modeled PM10 concentrations averaged over 11 remote PM10 monitoring sites. The blue underlines designate periods with the dust events.

Fig. 6. Time series of measured PM10 concentration (stars) and modeled PM10 concentration simulated by TCAM with DREAM boundary conditions (solid line) and without DREAM (dashed line). The data were averaged over 230 PM10 monitoring sites. The blue underlines designate periods with the dust events.

Fig. 7. Comparison of 95th percentiles between measured and modeled PM10 concentration during the dust events, simulated by TCAM with DREAM boundary conditions (TCAM+DREAM) and without DREAM (TCAM).

Fig. 8. Box plots of two indices of model performance: (a) the median of correlation, and (b) the median of normalized mean absolute error, computed on the basis of model-vs.-measurement comparisons at 230 PM10 monitoring sites. The performance of two model configurations is compared: TCAM with DREAM boundary conditions (TCAM+DREAM) and the base TCAM model (TCAM).

Fig. 9. Maps of differences in (a) correlation and in (b) normalized mean absolute error based on two model simulations with and without the DREAM boundary conditions. (blue: noticeably decreasing (< -0.1), red: noticeably increasing (> 0.1), green: almost unchanged).

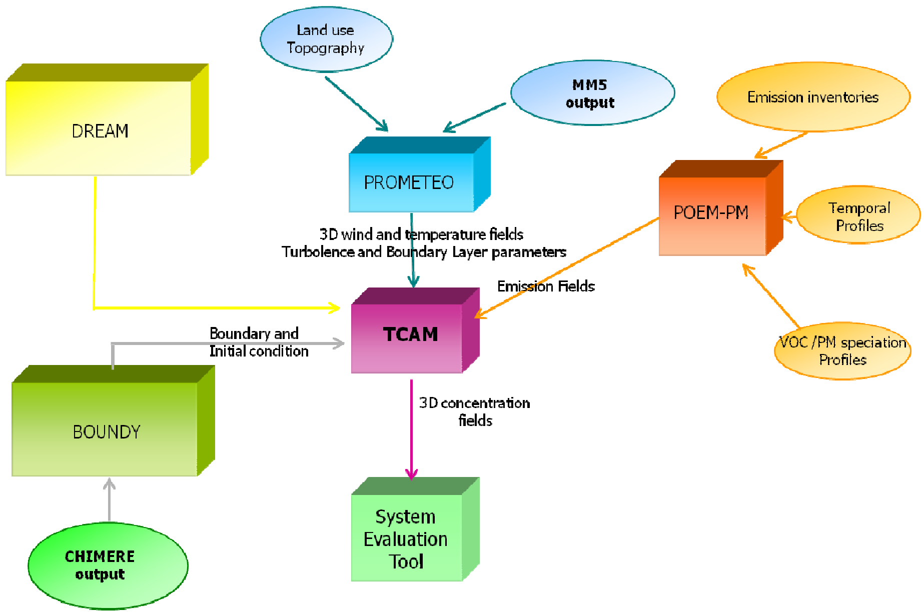

Fig. 1. The TCAM model configuration with embedded DREAM dust forecasts.

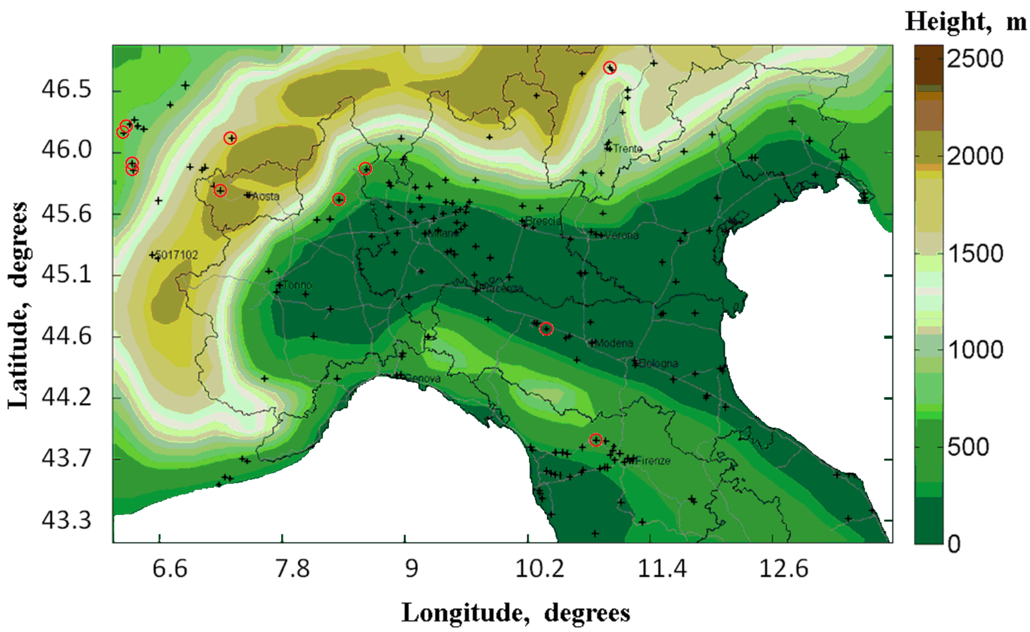

Fig. 2. The Northern Italy model domain with PM10 monitoring sites (crosses). The red rings designate the remote PM10 sites with the lowest average PM10 concentration.

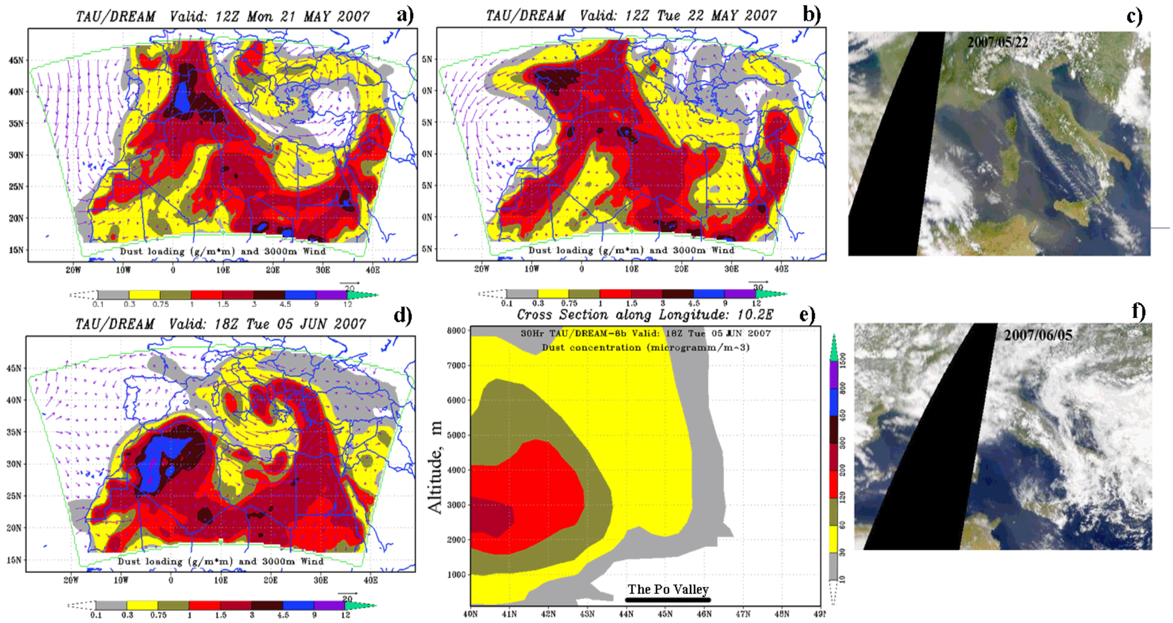

Fig. 3. DREAM dust forecasts and SeaWIFS satellite images of Saharan dust transport to Northern Italy in the first (top) and second (bottom) dust events. In Fig. 3 a, b, and d the colors designate dust loading in g/m^2, while in Fig. 3e the colors designate dust concentration in $\mu g/m^3$ within the vertical cross-section along the 10.2^o longitude. Wind vectors designate wind at 3000 m altitude.

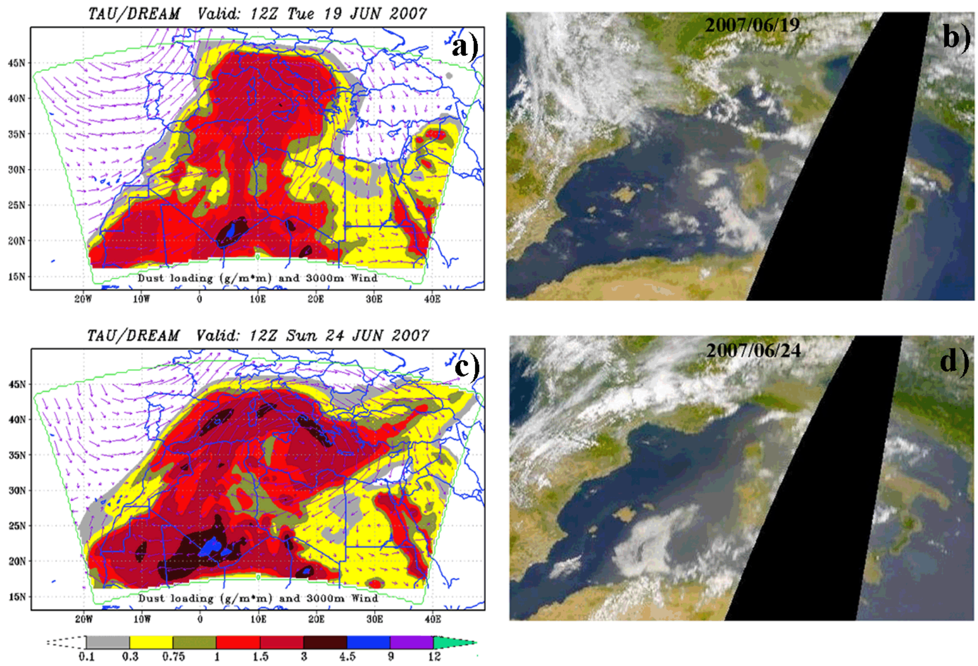

Fig. 4. DREAM dust forecasts (left panel) and SeaWIFS satellite images of Saharan dust transport to Northern Italy: (a and b) June 19, 2007, and (c and d) June 24, 2007. In the left panel, the colors designate dust loading in g/m^2, while wind vectors designate wind at 3000 m altitude.

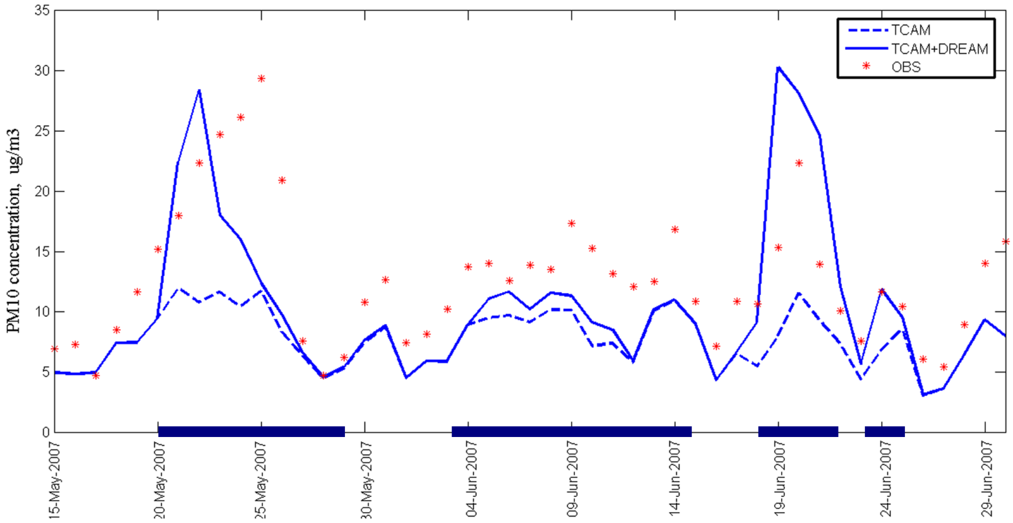

Fig. 5. Time series of measured and modeled PM10 concentrations averaged over 11 remote PM10 monitoring sites. The blue underlines designate periods with the dust events.

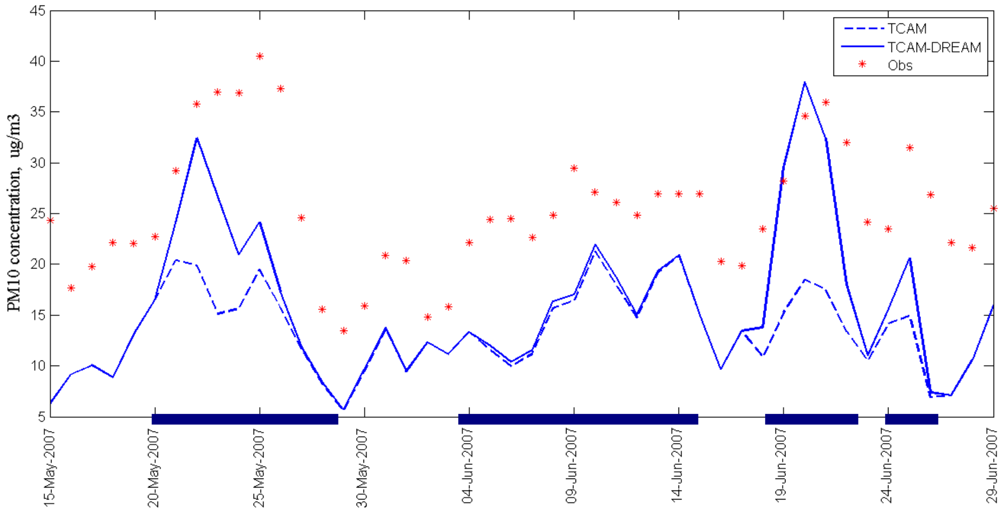

Fig. 6. Time series of measured PM10 concentration (stars) and modeled PM10 concentration simulated by TCAM with DREAM boundary conditions (solid line) and without DREAM (dashed line). The data were averaged over 230 PM10 monitoring sites. The blue underlines designate periods with the dust events.

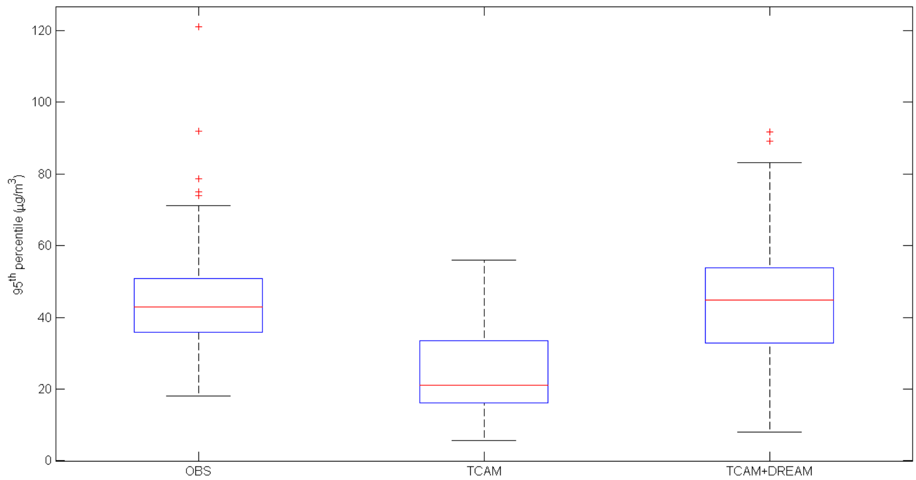

Fig. 7. Comparison of 95^{th} percentiles between measured and modeled PM10 concentration during the dust events, simulated by TCAM with DREAM boundary conditions (TCAM+DREAM) and without DREAM (TCAM).

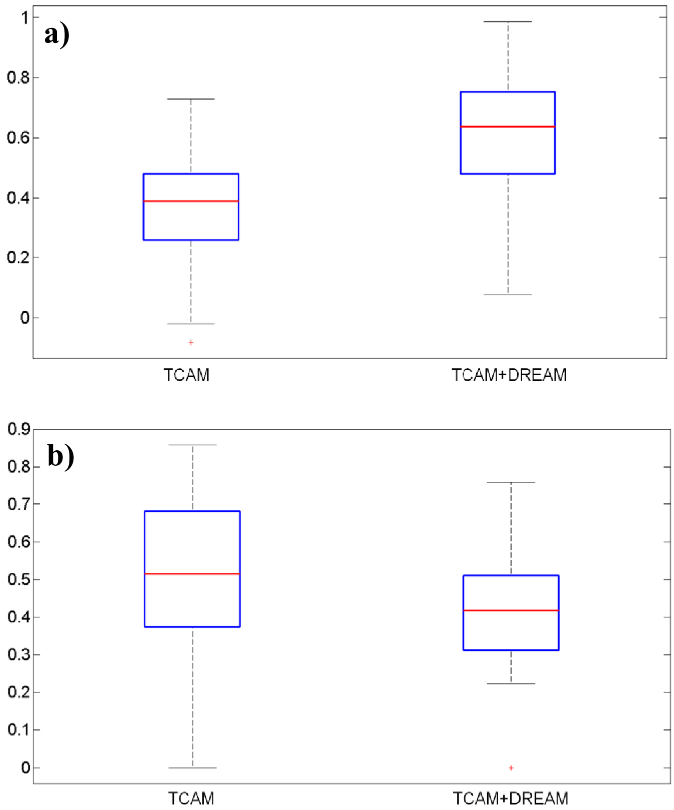

Fig. 8. Box plots of two indices of model performance: (a) the median of correlation, and (b) the median of normalized mean absolute error, computed on the basis of model-vs.-measurement comparisons at 230 PM10 monitoring sites. The performance of two model configurations is compared: TCAM with DREAM boundary conditions (TCAM+DREAM) and the base TCAM model (TCAM).

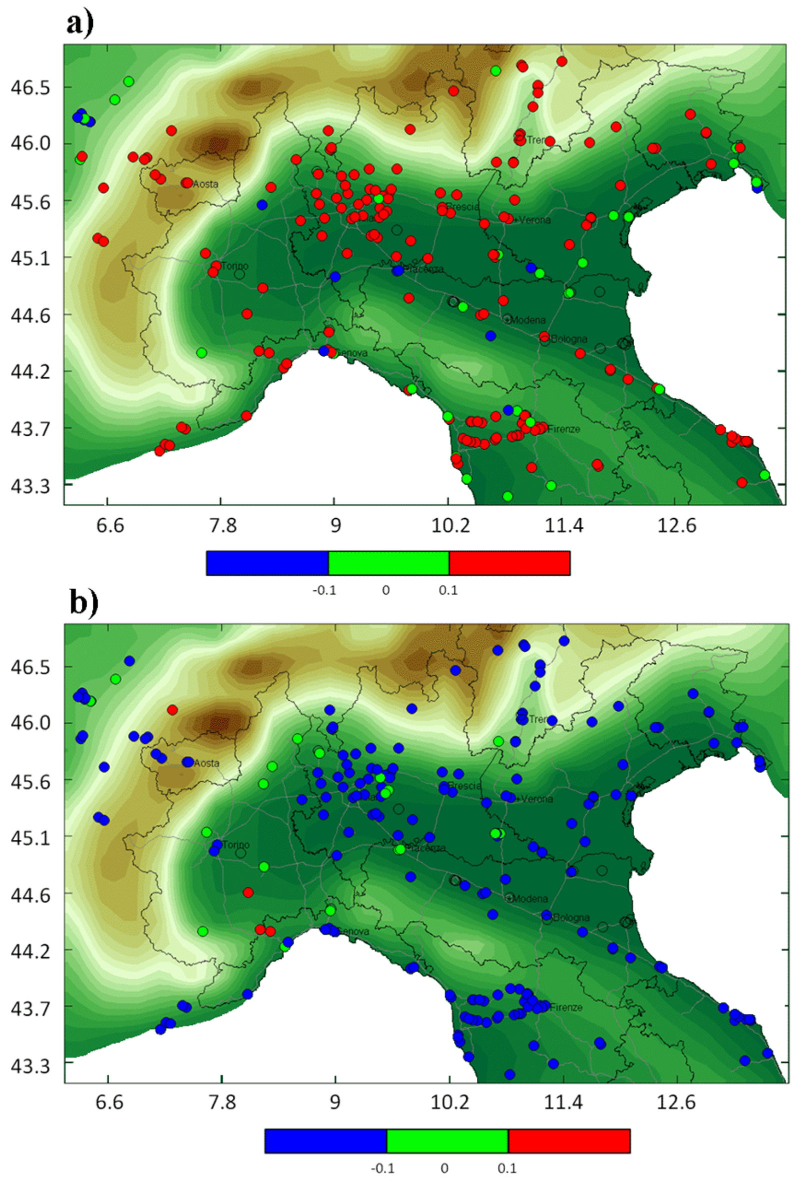

Fig. 9. Maps of differences in (a) correlation and in (b) normalized mean absolute error based on two model simulations with and without the DREAM boundary conditions. (blue: noticeably decreasing (< -0.1), red: noticeably increasing (> 0.1), green: almost unchanged).